Asia-Pacific Journal of Science and Technology :Volume :30 Issue :06 Article ID :APST-30-06-03 Research Article

APST

Asia-Pacific Journal of Science and Technology

https//:www.tci-thaijo.org/index.php/APST/index

Published by Research and Innovation Department,
Khon Kaen University, Thailand

In vitro anti-leukemic activity of *Terminalia arjuna* bark extract loaded chitosan nanoparticles on HL-60 cell lines

Gokul Murukadas[1], Anju Rani George[1], Hansiya V S[1], Sradha Sajeev[1], Kavimani Thangasamy[1], Aarthi Jeganathan[1], Anju Byju[1] and Natesan Geetha[1*]

[1] Department of Botany, Bharathiar University, Coimbatore – 641 046
[*]Corresponding author: geetha@buc.edu.in

Received 27 July 2024
Revised 18 April 2025
Accepted 11 June 2025

Abstract

The bark of *Terminalia arjuna* (Roxb. ex DC.) Wight & Arn. has been traditionally used in Indian medicine for treating various ailments, including leukemia. Chitosan, a natural biopolymer, serves as a promising carrier for targeted drug delivery. This study focuses on the encapsulation of hexane-ethanolic bark extract (HEB) of *T. arjuna* using chitosan nanoparticles (CSNPs) and evaluates their anti-leukemic potential against HL-60 cell lines. The HEB-loaded CSNPs (HEB-CSNPs) were synthesized and their entrapment efficiency, drug release profile and cytotoxic activity were assessed. *In vitro* release studies demonstrated a controlled and sustained drug release of 96.66% within three hours. Drug release kinetics followed the Higuchi model with a correlation coefficient (R^2) of 0.98, indicating diffusion-controlled release. Fourier transform infrared (FTIR) spectra confirmed the presence of characteristic functional groups of both chitosan and the plant extract. X-ray diffractometer (XRD) analysis revealed an increase in nanoparticle size from 56.88 nm (control) to 64.53 nm upon encapsulation. Search engine marketing (SEM) imaging showed well-dispersed nanoparticles with a large surface area. Cytotoxicity analysis on HL-60 cells demonstrated dose-dependent activity, with an inhibitory concentration (IC) IC_{50} value of 185.2 µg/mL for HEB-CSNPs. *Conclusion*: Overall, this study demonstrates that CSNPs are effective carriers for *T. arjuna* bark extract, ensuring efficient encapsulation, sustained release, and significant anti-leukemic activity *in vitro*. These findings suggest the potential of HEB-CSNPs as a biocompatible and eco-friendly nanomedicine for leukemia treatment and warrant further investigation in preclinical models.

Keywords: Chitosan nanoparticles, *Terminalia arjuna*, Cytotoxicity, HL-60 cell lines, *In vitro* drug release kinetics, Leukemia cancer

1. Introduction

Leukemia, a hematopoietic cancer that results from the malignant transformation of white blood cells and it is one of the most common types of cancer worldwide [1]. Its etiology includes genetic alterations, environmental influences, smoking, alcohol consumption, chemicals, ionizing radiation and immune deficiencies. Although chemotherapy and radiation are standard treatments, their severe side effects and dose-limiting toxicity often lead patiets to seek plant-based alternatives with fewer adverse effects [2,3]. Several types of ethno-medicinal plants have been used to treat leukemia. For example, two alkaloids such as homoharringtonine and harringtonine isolated from *Cephalotaxus harringtonia* are reported to possess anti-leukemic effects. Vinca alkaloids of *Catharanthus roseus* such as vinblastine and vincristine are used to treat leukemia. Maytansinoid, a benzoansamacrolide isolated from the bark of *Maytenus serrate* has a potential anticancer activity [4]. Vernodaline and vernolide, sesquiterpene lactone compounds isolated from root extract of *Vernonia amygdaline* are involved in killing abnormal cells by promoting cell apoptosis. Leaf and seed extracts of *Annona glabra* inhibit the leukemic cell colony formation [5].

Nanotechnology is a new science dealing between 1 and 100 nm sized particles that have at least one dimension less than 100 nm in size [6]. Nanoparticles, classified as organic or inorganic, are valued for their stability under adverse conditions. Polymeric nanoparticles, especially those derived from natural biopolymers like polysaccharides and proteins, have gained significant interest in pharmaceuticals due to their biocompatibility, biodegradability, and potential in drug delivery and therapeutic applications [7]. Recently, preparation of natural polymer based nanocarrier has been in the focus of various nanotechnology research. Among all the natural polymers, chitosan plays an imperative role in tissue engineering, nano-drug delivery systems and surgical/medical devices due to their reduced size, better stability, non-toxic, eco-freindly nature, least expensive, simple and mild preparation methods.

Terminalia arjuna (Roxb.), is a large woody plant, locally known as *'Arjuna'* belonging to the family Combretaceae. Cardio protective property of this plant has been mentioned in many ancient Indian medicinal literatures including Charaka Samhita and Astang Hridayam [8]. Other than this property, the plant also possess antioxidant, hypotensive, antiatherogenic, antiinflammatory, anticarcinogenic, anti-mutagenic and gastro-productive properties. Triterpenoids are found in stem bark, roots and fruits and glycosides are present in stem bark, roots and leaves. Stem bark, flower and leaves possess flavonoids. Tannins are present only in the stem bark [9]. Bark extract shows many properties such as hypocholesterolemic, hypolipidemic, antioxidative, antimutagenic, antibacterial, antiviral and antitumor [10]. Ethanolic bark extract induced cytotoxicity in human hepatoma cells, petroleum ether bark extract in liver and colon cancer cell lines [11], aqueous extract of bark showed cytotoxicity effect on lung and breast cancer cell lines and on mice bearing mammary tumors [12] and alcoholic bark extract exhibited cytotoxic property on human T-lymphoblastic cell lines [13]. Recently, using bark extract of *T. Arjuna*, selenium nanoparticles were synthesized, characterized and used for analysis of their antioxidant, antibacterial, anticancer (breast cancer) activities along with formulation of gel by incorporating the synthesized nanoparticles [14]. There has been no information on encapsulation/loading of bark extract of *T. arjuna* onto chitosan nanoparticles and evaluation of their cytotoxic potential against cancer cell lines. Therefore, the present study aims to fill the gap by investigating the anti-leukemia potential of *T. arjuna* bark extract-loaded chitosan nanoparticles.

2. Materials and methods

2.1 Chemicals

Medium molecular weight chitosan (190-310 kDa MW with 75-85% degree of deacetylation) and dialysis membrane bags were purchased from Sigma-Aldrich. Glacial acetic acid, Sodium tripolyphosphate and phosphate buffer (pH 7.4) were purchased from Sisco Research Laboratories Pvt. Ltd., Mumbai, India.

2.2 Collection, identification and processing of plant material

The bark of *T. arjuna* was collected from Maruthamalai hills, Coimbatore district, Tamil Nadu. Taxonomic identification and authentication were done by Department of Botany, Bharathiar University, Coimbatore. Bark samples were collected from mature plant and cut into small pieces and washed under running water to remove adhering debris. Then the samples were dried under shade and ground into fine powder and stored at 4°C.

2.3 Bark extraction

120 gm of powdered bark sample was macerated over 48 hrs in two litres of hexane at 30°C. Hexane extract was filtered using whatman No.1 filter paper and the filtrate was macerated with 70% ethanol. Hexane-ethanolic bark (HEB) flltrate was dried at room temperature and used for further analysis.

2.4 Formulation of Hexane-ethanolic bark encapsulated chitosan nanoparticles (HEB-CSNPs)

HEB-CSNPs were prepared following the ionic gelation method [15]. Briefly, 0.5% (w/v) chitosan was taken and dissolved in 1% glacial acetic acid and stirred until it was transparent. Then, the pH was adjusted to 5.0 at room temperature. 100 µg/mL HEB was added to various concentrations of chitosan nanoparticles (CSNPs) (10, 20, 30, 40, 50 µg/mL) Then, 0.1% the sodium tripolyphosphate solution (TPP) was added dropwise to the mixture and stirred until the opalescent formation. The mixture was centrifuged at 10000 rpm for 15 min and washed twice with deionized water, after centrifugation, the supernatant was discarded and pellet containing HEB-CSNPs was stored in the refrigerator at 4°C for further use.

2.5 Entrapment Efficiency Percent (EE%)

The amount of HEB encapsulated/entraped within the CSNPs was determined by indirect method, through calculating the amount of unencapsulated drug. After adding the TPP, the mixture was centrifuged at 10000 rpm for 15 min and the clear supernatant containing the free unencapsulated drug was collected, diluted with distilled water and measured spectrophotometrically at 273 nm [16]. The drug HEB entrapment or encapsulation efficiency in CSNPs was determined using the following equation.

$$EE\% = \frac{Total\ amount\ of\ HEB\ added - Free\ HEB\ in\ supernatant}{Total\ HEB\ added} \text{ X } 100 \quad (1)$$

2.6 Estimation of in vitro drug release percentage

HEB release percentage from CSNPs was determined using the technique of dialysis tube analysis (12,000-14,000 molecular weight). In brief, the dialysis membrane was washed with lukewarm double distilled water (70ºC) for 1 hr and rinsed thoroughly (thrice) to eliminate glycerine. HEBCSNPs with higher entrapment efficiency (95.6) was placed in a dialysis bag which was sealed and immersed in 50 mL of phosphate buffer (pH 7.4) at room temperature with stirring at 1000 rpm for 6 h. 3 mL of the solution was withdrawn every half an hour and replaced with an equivalent volume of fresh solution. This process was repeated upto 3.5 hours. The withdrawn samples were analyzed using UV/visible spectroscopy at 265 nm and the amount of HEB release pattern from CSNPs was determined [17]. The drug release percentage was determined by using the following formula.

$$Drug\ release\ (\%) = \frac{C(t)}{C(0)} \text{ X } 100 \quad (2)$$

where *C(t)* is the absorbance of HEB-CSNPs at 265 nm at time t.

2.7 In vitro drug release kinetics

Various kinetic models such as zero order, first order, Higuchi model and Korsmeyer–Peppas have been applied to fit the cumulative *in vitro* drug release data and to describe the drug release kinetics [18]. The best release pattern is explained using the coefficient of determination (R^2) value. Model with the highest R^2 is considered as the best one [19].

2.8 Characterization of drug loaded chitosan nanoparticles

HEB-CSNPs were subjected to UV-vis spectrophotometry and Fourier transform infrared spectroscopy (FTIR) to study optical properties and to identify functional groups, respectively. Detection of topography and particle size of chitosan encapsulated HEB was investigated through Scanning electron microscopy (Quanta 400 ESEM) and X-ray diffractometer (Shimadzu LabX- XRD 1600), respectively. The physical stability of nanoparticles was assessed using zeta potential analyzer (Malvern Panalytical, Chennai India).

2.9 In vitro anti-leukemic activity

Human acute promyelocytic leukemia cell lines (HL-60) were obtained from american type culture collection (ATCC) 10801. Cells were cultured in dulbecco's modified eagle medium (DMEM) media supplemented with 10% (*v/v*) feta lbovin serum and 1% (*v/v*), 100 U/mL penicillin and 100 µg/mL streptomycin. Cells were cultured in an incubator at 37°C and 5% CO_2 humidified atmosphere. Medium was changed every 2 -3 days. Reagents and media for cell culture were sourced from Sigma-aldrich (Merck) and Sisco Research Laboratories Pvt. Ltd., Mumbai, India.

The cellular toxicity on cultured cells was measured using 3-(4,5-dimethylthiazol-2-yl)-2, 5-diphenyl tetrazolium bromide (MTT) assay. Cells were grown overnight in a 96-well plate at a density of 1×10^4 cells per well. Then, cells were treated with different concentrations of test samples such as HEB and HEB-CSNPs (0, 10, 20, 40, 80, 160 and 320 µg/mL), anticancer agent Doxorubicin (3.125, 6.25, 12.5, 25, 50, 100µM) and incubated at 37°C for 24 h. Later, cells were washed twice with phosphate buffer saline (PBS). MTT solution was added to each well (0.5 mg/mL) and the plate was incubated for 4h at 37° C in 5% CO_2 atmosphere. Finally, the medium was replaced with DMSO to solubilize the formazan and absorbance was measured at 590nm using a microplate reader. IC_{50} value for cytotoxicity tests were derived from a nonlinear regression analysis based sigmoid dose response curve and calculated using prism Graph Pad Prism 6 (Graph pad, SanDiego, CA, USA) [20]. The percentage growth inhibition was calculated using the following formula

$$\% \, inhibition = \frac{control \; abs - sample \; abs}{control \; abs} \text{ X } 100 \qquad (3)$$

2.10 Light microscopy observation

The effect of HEB and HEB-CSNPs on HL-60 cell lines was monitored using light microscope. For this, the treated cell lines (HEB-CSNPs and standard) along with control HEB were prepared in a 96-well plate and incubated for 24, 48 and 72 hr. After incubation, the morphological changes of cell lines were observed under microscope.

3. Results and Discussion

3.1 Preparation of chitosan nanoparticles (CSNPs) and formulation of HEB encapsulated nanochitosan

Using ionic gelation method, CSNPs were produced in the form of a hydrogel and stabilized through electrostatic interactions of the amino group of cationic chitosan (NH_3) and the polyanion group (O) of anionic crosslinking agent, usually TPP. When HEB extract was added to CSNPs, the color of the mixture changed from red colour to brown colour indicating the encapsulation of HEB onto CSNPs i.e. HEB-CSNPs (Figure 1) which was in agreement with the report of El-Naggar *et al.* (2023) [21].

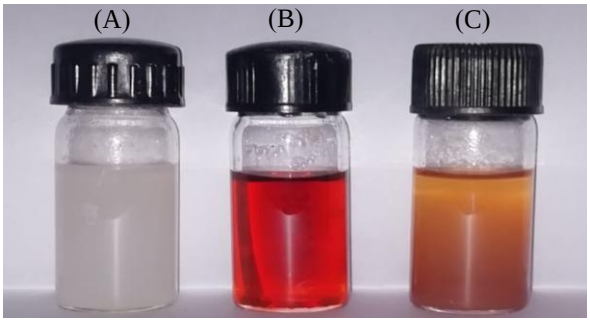

Figure 1 Formulation of HEB encapsulated nanochitosan. (A) Vial of CSNPs solution, (B) vial of HEB extract of *T. arjuna*, (C) vial of HEB encapsulated CSNPs.

3.2 Encapsulation/Entrapment Efficiency Percent (EE%)

Encapsulation of HEB (100 µg/mL) in CSNPs was carried out at different concentrations of CSNPs i.e. 10, 20, 30, 40, and 50 µg/mL. Among various concentrations of CSNPs, 20 µg/mL CSNPs showed higher encapsulation efficiency (95.6%) with HEB (Figure 2). Increasing the concentration of CSNPs caused a decrease of EE% from 30 to 50 µg/mL CSNPs due to the limited encapsulation capacity and saturation of particles with HEB. Similar results have been reported in previous studies entrapping ascorbyl palmitate, quercetin, thyme essential oil, krill oil of *Euphausia superba* and aqueous grape extract [22].

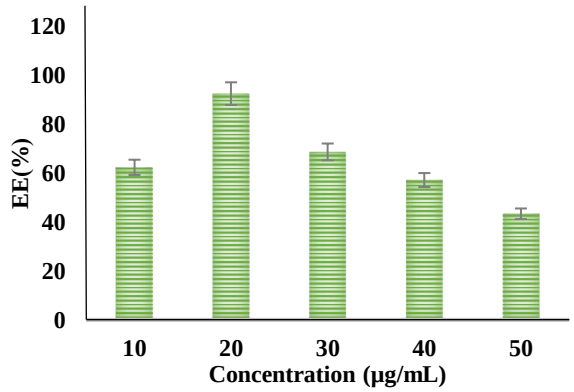

Figure 2 Encapsulation efficiency percentage of HEB-CSNPs at different concentration of CSNPs.

3.3 In vitro drug release study

The cumulative release of the HEB from CSNPs was studied in dialysis bag containing PBS solution at pH 7.4. The released amount of HEB was calculated by comparing the absorbance of the drug at 265 nm by UV–vis spectroscopy with the earlier measured calibration curves with a dilution series. Finally, the cumulative percent of drug released from CSNPs was plotted against time [23]. *In vitro* drug release studies demonstrated a controlled and sustained release of HEB from nanochitosan (96.66%) within three hours.

3.4 In vitro drug release kinetics

In order to analyze the *in vitro* release data and to evaluate the drug release kinetics, four mathematical models such as zero order, first order, Higuchi model and Korsmeyer–Peppas have been used. The mechanism of drug release from CSNPs involves (A) release of adsorbed or entrapped drug in the surface layer of particles; (B) diffusion through the swollen polymermatrix and (C) long-term drug release due to polymer erosion, breakdown, hydrolysis or degradation of the NPs backbone [24]. The drug release kinetics from drug carrier is essential in preclinical development and will serve as the foundation for evaluation of drug formulations and regulatory approvals. Prediction of *in vivo* drug release through *in vitro* techniques for nano-formulations is becoming extensively developed [25]. The diffusion-controlled release kinetics was investigated using the zero-order, first-order, and Higuchi models. Mathematical models have many advantages, including predicting drug release mechanisms, helping in formulation development, and fabricating controlled drug release systems [26]. Figure 3 shows correlation coefficient values (R^2) from the model fitting of the release profiles. The Higuchi model yielded the highest R^2 value (0.94) compared to the other models. This result suggested that HEB release at pH 7.4 from HEB-CSNPs complex follows the Higuchi model kinetics. It also indicates that HEB is released by diffusion process [27].

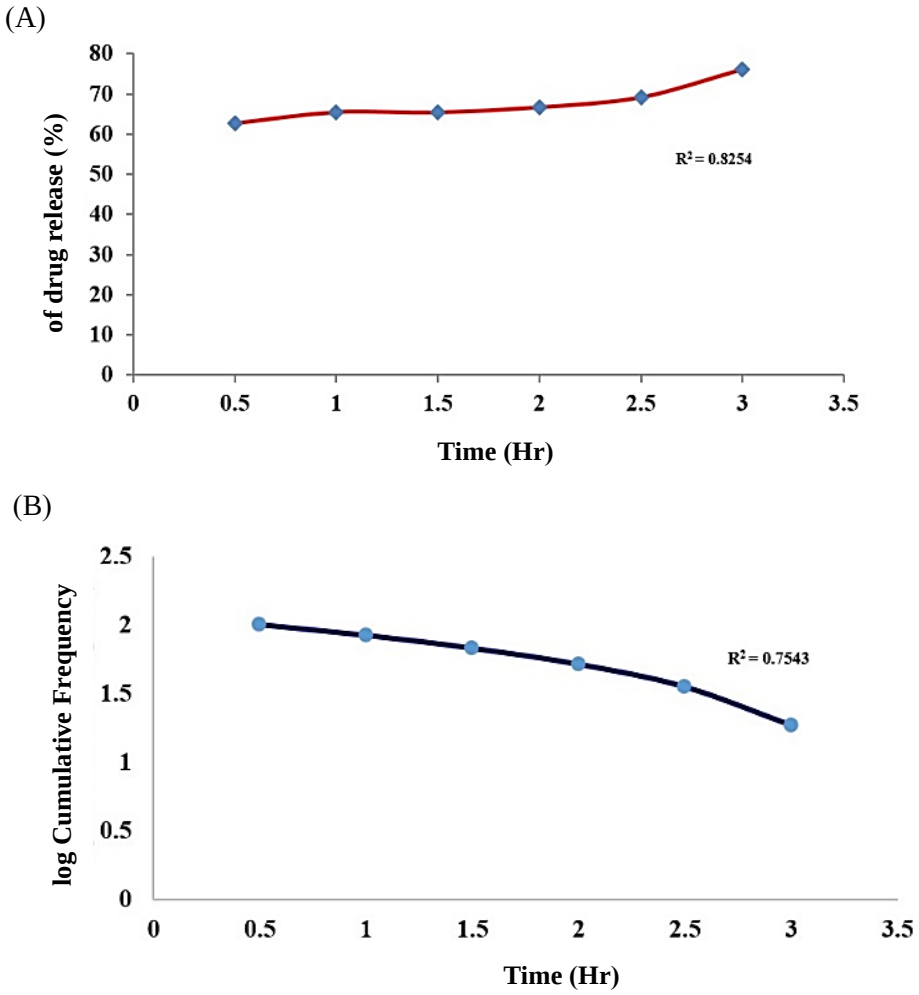

Figure 3 *In vitro* drug release kinetics (A) Zero order kinetics, (B) First order kinetics, (C) Higuchi model, (D) Korsmeyer-peppas model.

(C)

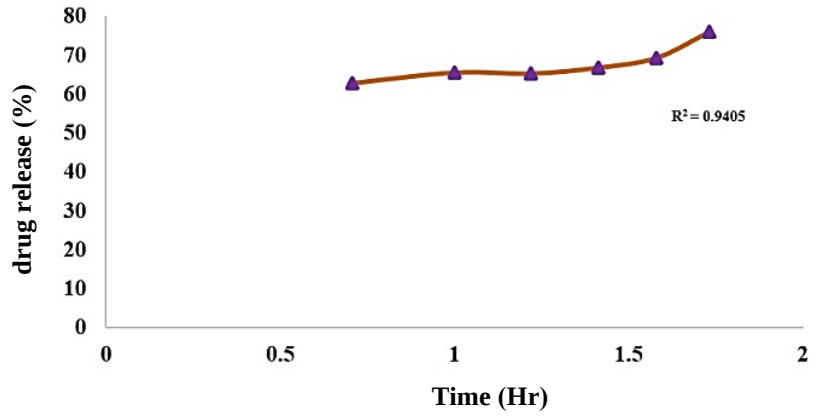

(D)

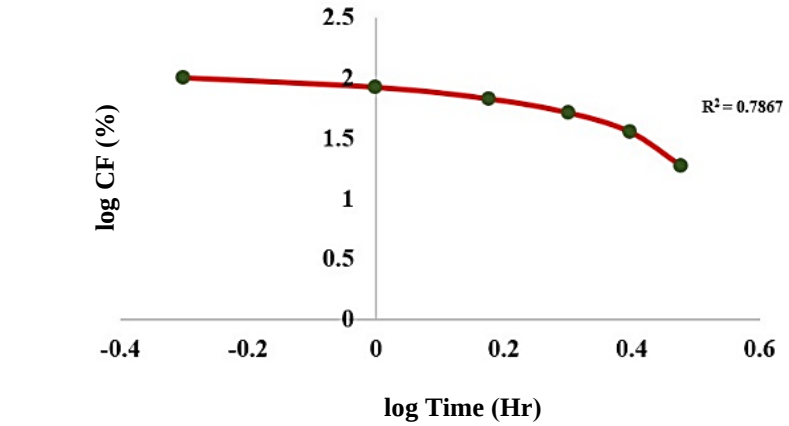

Figure 3 (cont.) *In vitro* drug release kinetics (A) Zero order kinetics, (B) First order kinetics, (C) Higuchi model, (D) Korsmeyer-peppas model.

3.5 Characterization of HBE-CSNPs

To identify the absorbance peaks of both CSNPs and HEB-CSNPs, a UV/Vis spectrophotometer scans were taken over the wavelength range of 200 to 800 nm. The strong surface plasmon resonance (SPR) centered at 250 nm was attributed to both CSNPs and HEB-CSNPs. It was earlier reported that the UV–visible spectrum of chitosan nanoparticles was ranged between 200 and 322 nm due to the presence of the C=O functional group [28]. The present findings are in agreement with those of El-Naggar *et al* (2023) [36] who loaded *Lavendula angustifolia* leaves extract onto chitosan nanoparticles and obtained peak at 285 nm for both CSNPs and leaf extract loaded CSNPs.

FTIR analysis was carried out to identify functional groups present in the HEB-CSNPs complex. FTIR spectrum of HEB-CSNPs is compared with the FTIR spectrum of CSNPs (Figure 4 (A) and (B)). In the FTIR spectrum of CSNPs, the prominent peak values are found to be 3194.51 cm (OH and NH stretchings), 2883.18 cm (asymmetric C-H stretching), 1632.94 cm (C=O and C=C stretching), 1534.11 cm (N-H deformation) and 1385.86 cm (C-O and C-F stretchings). HEB-CSNPS complex shows major peaks at 3219.75 cm 2885.66 cm, 1620.57 cm, 1532.58 cm and 1378.45 cm. However, the significant shift of the peaks in the spectrum of HEB-CSNPS complex indicate an important role of various functional groups of CSNPs in the successful of encapsulation of HEB onto chitosan nanoparticles. The broad bands (3219.75 cm and 2885.66 cm) and narrow bands (1620.57 cm, 1532.58 cm and 1378.45 cm) in HEB-CSNPs complex compared to CSNPs indicate the new intermolecular hydrogen bond interaction formed between these complexes [29].

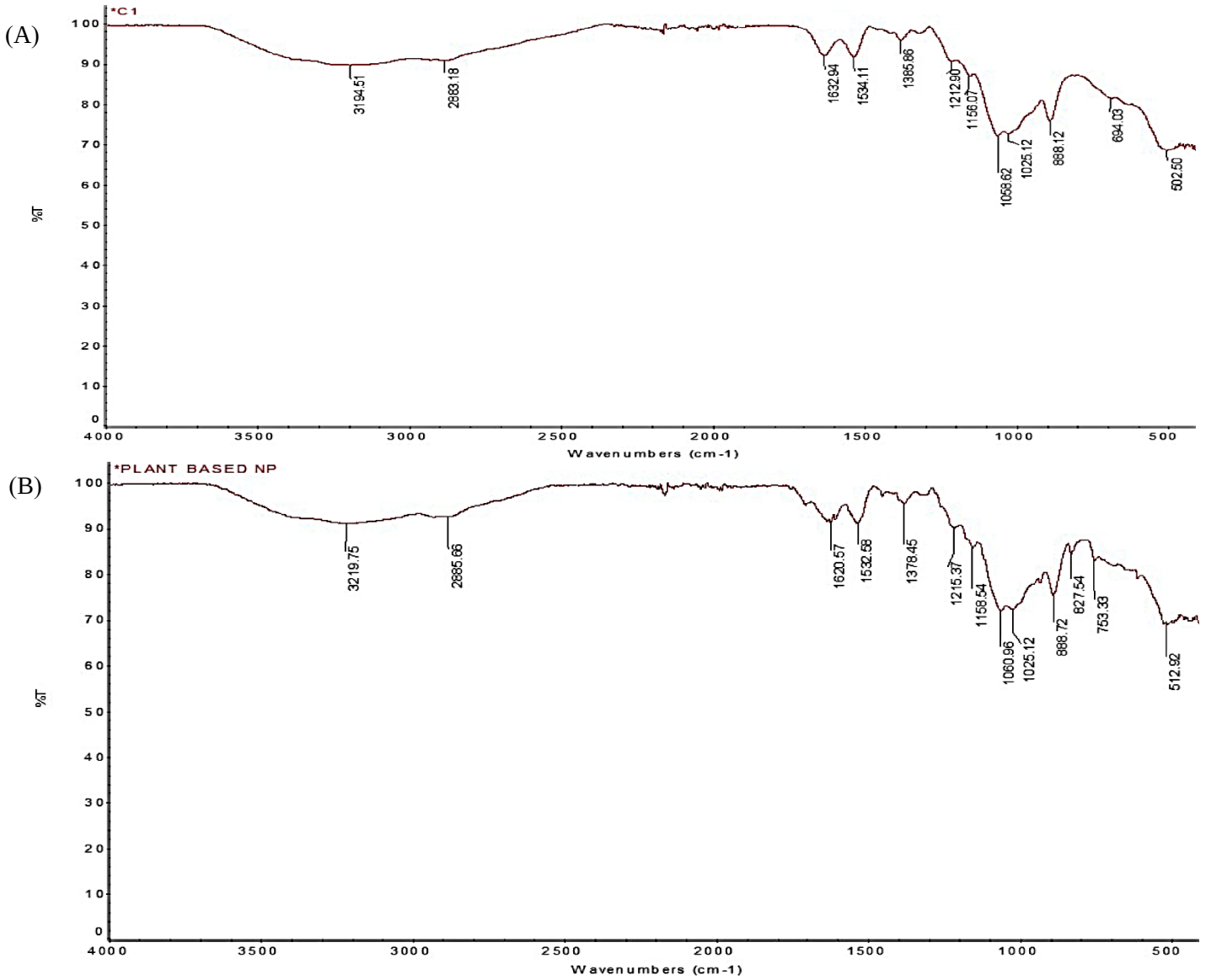

Figure 4 FTIR spectrum of (A) CSNPs, (B) HEB-CSNPs complex; X-ray diffraction pattern of (C) CSNPs and (D) HEB-CSNPs complex; 3 SEM analysis micrograph image (A) CSNPs and (B) HEB-CSNPs complex.

(C)

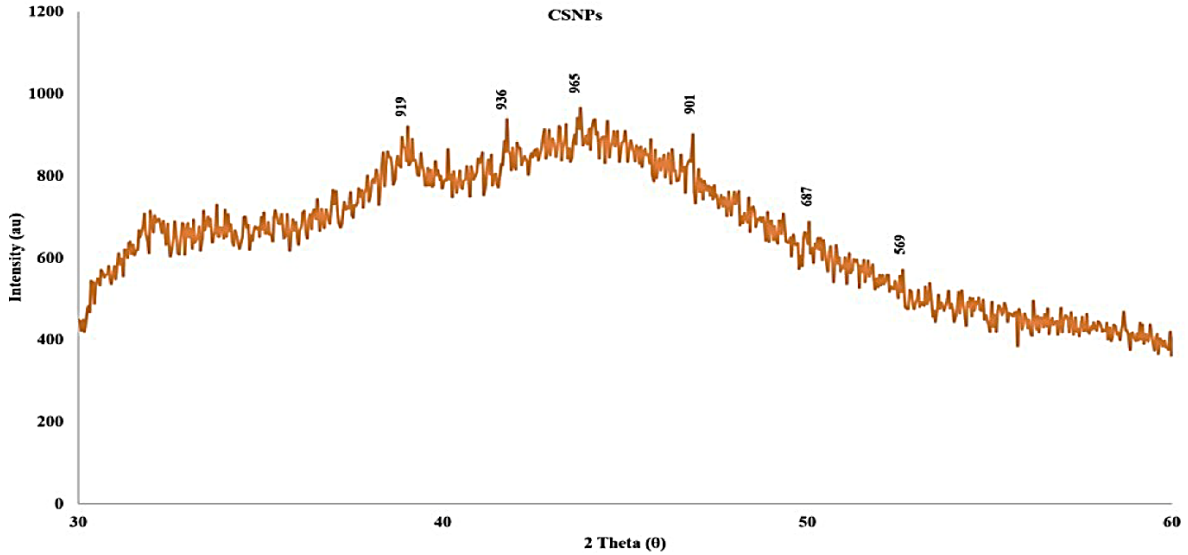

(D)

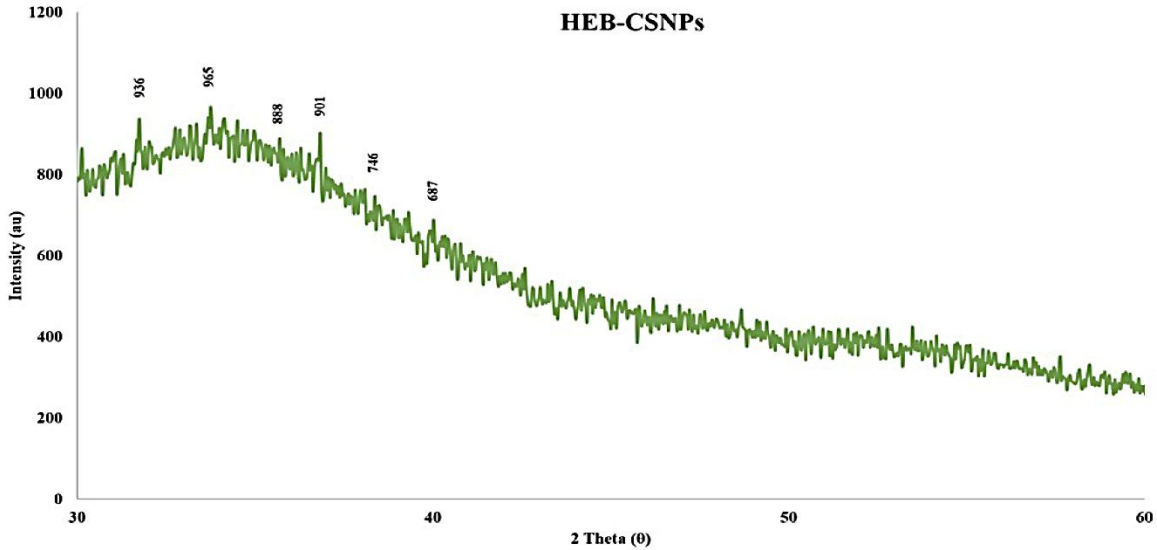

Figure 4 (cont.) FTIR spectrum of (A) CSNPs, (B) HEB-CSNPs complex; X-ray diffraction pattern of (A) CSNPs and (B) HEB-CSNPs complex; SEM analysis micrograph image (E) CSNPs and (F) HEB-CSNPs complex

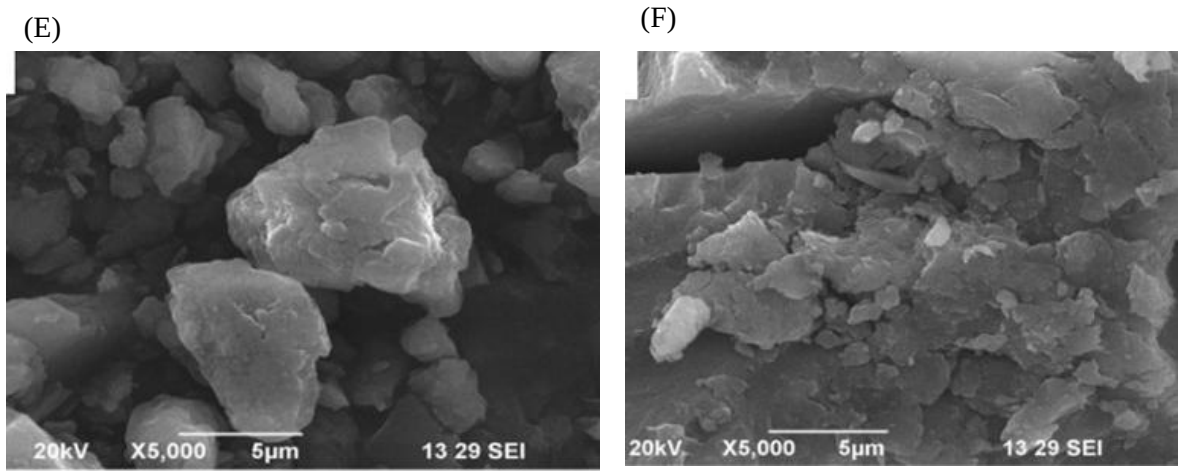

Figure 4 (cont.) FTIR spectrum of (A) CSNPs, (B) HEB-CSNPs complex; X-ray diffraction pattern of (C) CSNPs and (D) HEB-CSNPs complex; SEM analysis micrograph image (E) CSNPs and (F) HEB-CSNPs complex.

X-ray diffraction analysis was performed to compare the crystalline structure of CSNP and HEB-CSNPs complex (Figure 4 (C) and (D)). CSNPs exhibits one broad peak at 2θ = 21.63° whereas and HEB-CSNPs shows the characteristic peak found at 2θ = 26.28° with significant degree of amorphous phase [30]. Chitosan nanoparticles are comprised of a dense network structure of interpenetrating polymer chains crosslinked to each other by TPP counter ions [31]. When compared with CSNPs, diffraction spectrum of drug encapsulated nanochitosan the characteristic peak found at 2θ (26.28°) confirming the presence of HEB within the chitosan nanoparticle [29].

The SEM images of CSNPs and HEB-CSNPs are shown in Figure 4 (E) and (F). With different magnification ranges, SEM images were taken. The surface morphology of CSNPs is similar to HEB-CSNPs. The size of crystalline structure was calculated using Debye–Scherrer equation. The mean size of CSNPs was found smaller (56.88) than the HEB loaded CSNPs (64.53nm). The addition of HEB to CSNPs makes the size of CSNPs to enlarge. These results are found comparable with the findings of previous researchers [32].

The cytotoxicity of both HEB and HEB-CSNPs were investigated against Human Leukemia cell line (HL–60). Results indicated that HEB-CSNPs have more cytotoxic activity on HL-60 cell lines compared to HEB. The calculated IC $_{50}$ values based on MTT cell viability assay for HEB and HEB-CSNPs are found to be 209.3 µg/mL and185.1 µg/mL, respectively (Figure 5). The positive control Doxorubicin showed 17.08 µM IC_{50} value. The results showed the percentage of inhibition of cell proliferation increases with increase in concentration and dose dependent manner for HEB and HEB-CSNPs [52].

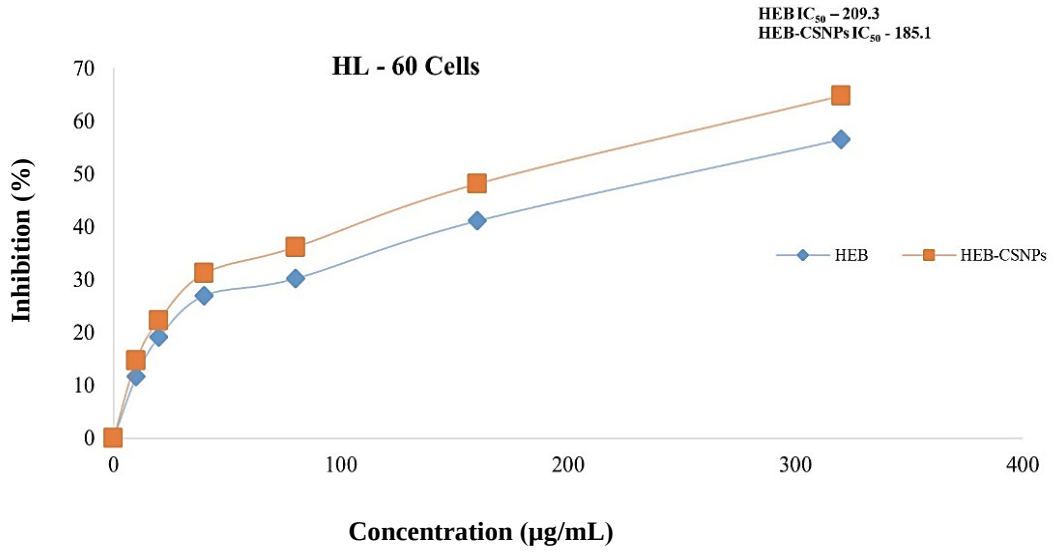

Figure 5 Cytotoxicity effect of HEB and HEB-CSNPs), against HL-60 cell lines after 24 -72 hours of incubation.

Figure 6 shows microscopic images of IC_{50} HEB and HEB-CSNPs along with standard against HL-60 cell lines. 24, 48 and 72 hr. HEB-CSNPs treated HL-60 cell lines exhibited the typical features of apoptosis, such as chromatin condensation, cell shrinkage and membrane blebbing compared to control (HEB treated cell lines). Apoptotic bodies formation was more prominent at 72 hr. after treatment of HEB-CSNPs than 24 and 48 hr. treated cell lines. These results were in line with other studies showing that cytotoxic activity of saponins isolated from the leaves of *Gymnema sylvestre* and *Eclipta alba* against HeLa cell lines and suppressing the growth of HL-60 myeloid leukemia cells using chitosan coated anthroquinone nanoparticles [53].

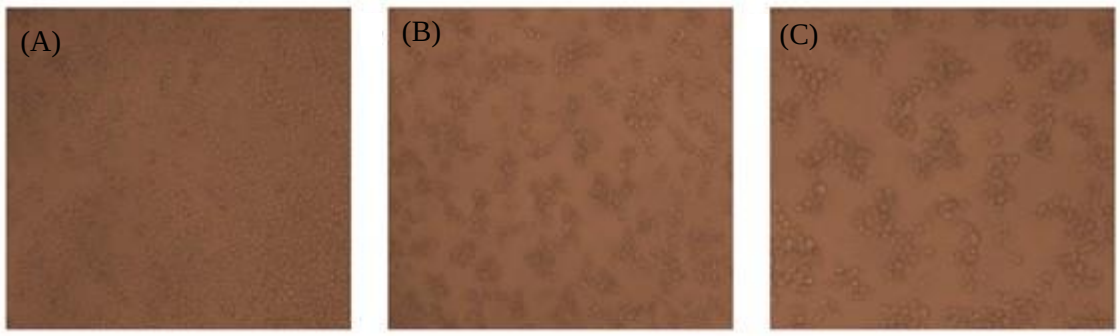

Figure 6 Morphological changes of HL-60 cells under light microscope after 78 hrs of incubation with (A) HEB, (B) HEB-CSNPs complex, (C) Doxorubicin.

4. Conclusions

In conclusion, the results clearly indicate the capability of CSNPs for loading *T. arjuna* bark extract efficiently with a steady *in vitro* drug release and its anti-leukemic potential against HL-60 cell line. For this, CSNPs were prepared *via* ionic gelation method and made to encapsulate HEB extract of *T. arjuna*. Among various concentrations of HEB-CSNPs, 20 µg/mL showed the highest entrapment efficiency. *In vitro* drug release studies showed a controlled and sustained release of HEB from nano chitosan within three hours. In this investigation, HEB release kinetics from CSNPs was found to be best fitted to the Higuchi model. Various spectroscopic studies confirmed the encapsulation of HEB onto CSNPs successfully. Superior cytotoxic activity was found against leukemia cell line by HEB-CSNPs complex than HEB which may be due to the presence of active phytocompounds of *T. arjuna* and also due to the electrostatic ionic interaction between the negatively charged groups of cancer cells and the positively charged amino groups of chitosan. Thus, these results strongly demonstrate the ecofriendly chitosan loaded drug could be used to treat leukemia cancer.

5. Acknowledgements

Authors sincerely acknowledges the financial support received from the RUSA 2.0 – BCTRC (Bharathiar Cancer Theranostic Research Centre, OM.No. BU/RUSA 2.0/2021/BCTRC/PG/R7/215-2 and all the instrumentation facilities provided from the Department of Botany, Bharathiar University, Coimbatore-641 046

6. References

[1] Saedi S, Moghaddam NS, Amerinatanzi A, Elahinia M, Karaca HE. On the effects of selective laser melting process parameters on microstructure and thermomechanical response of Ni-rich NiTi. Acta Mater. 2018;144:552-560.

[2] Mankaran S, Dinesh K, Deepak S, Gurmeet S. Typhonium falgelliforme: a multipurpose plant. Int Res J Pharm. 2013;4(3):45-48.

[3] Xu B, Ding J, Chen KX, Miao ZH, Huang H, Liu H, Luo XM. Advances in cancer chemotherapeutic drug research in China. Adv Cancer Res Ther. 2012;17:287-289.

[4] Vilpo JA, Koski T, Vilpo LM. Selective toxicity of vincristine against chronic lymphocytic leukemia cells in vitro. Eur J Haematol. 2000;65(6):370-378.

[5] Liu L, De Vel O, Han QL, Zhang J, Xiang Y. Detecting and preventing cyber insider threats: A survey. IEEE Commun Surv Tutor. 2018;20(2):1397-1417.

[6] Laurent S, Forge D, Port M, Roch A, Robic C, Vander Elst L, Muller RN. Magnetic iron oxide nanoparticles: synthesis, stabilization, vectorization, physicochemical characterizations, and biological applications. Chem Rev. 2008;108(6):2064-2110.

[7] Motiei M, Kashanian S, Lucia LA, Khazaei M. Intrinsic parameters for the synthesis and tuned properties of amphiphilic chitosan drug delivery nanocarriers. J Control Release. 2001;260:213-225.

[8] Amalraj A, Gopi S. Medicinal properties of terminalia arjuna (Roxb.) Wight & Arn.: a review. J Traditi Complementary Med. 2017;7(1):65-78.

[9] Dwivedi S, Udupa N. Terminalia arjuna: pharmacognosy, phytochemistry, pharmacology and clinical use. A review. 1989;60:413-420.

[10] Sivalokanathan S, Vijayababu MR, Balasubramanian MP. Effects of Terminalia arjuna bark extract on apoptosis of human hepatoma cell line HepG2. World J Gastroenterol 2006;12(7):10-18.

[11] Liu K, Newbury PA, Glicksberg BS, Zeng WZ, Paithankar S, Andrechek ER, Chen B. Evaluating cell lines as models for metastatic breast cancer through integrative analysis of genomic data. Nat commun. 2019;10(1):21-38.

[12] Greco G, Turrini E, Tacchini M, Maresca I, Fimognari C. The alcoholic bark extract of Terminalia arjuna exhibits cytotoxic and cytostatic activity on Jurkat leukemia cells. Venoms Toxins. 2021;1(1):56-66.

[13] Puri M, Gawri K, Dawar R. Therapeutic strategies for BRAF mutation in non-small cell lung cancer: a review. Front Oncol. 2023;13:1141-1876.

[14] Calvo P, Remunan-Lopez C, Vila-Jato JL, Alonso MJ. Novel hydrophilic chitosan-polyethylene oxide nanoparticles as protein carriers. J Appl Polym Sci. 1997;63(1):125-132.

[15] Bagyalakshmi J, Haritha H. Green synthesis and characterization of silver nanoparticles using Pterocarpus marsupium and assessment of its *in vitro* Antidiabetic activity. Am J Adv Drug Deliv. 2017;5(3):10-19.

[16] Sultan A, Ali R, Ishrat R, Ali S. Anti-HIV and anti-HCV small molecule protease inhibitors in-silico repurposing against SARS-CoV-2 Mpro for the treatment of COVID-19. J Biomol Struct Dyn. 2022; 40(23):12848-12862.

[17] Dash TK, Konkimalla VB. Poly-ϵ-caprolactone based formulations for drug delivery and tissue engineering: A review. J Control Release. 2012;158(1):15-33.

[18] Paarakh MP, Jose PA, Setty CM, Peterchristoper GV. Release kinetics–concepts and applications. Int J Pharm Res Technol. 2018;8(1):12-20.

[19] Lockwood JD, Aleksić JM, Zou J, Wang J, Liu J, Renner SS. A new phylogeny for the genus Picea from plastid, mitochondrial, and nuclear sequences. Mol Phylogenet Evol. 2013;69(3):717-727.

[20] Mazancová P, Némethová V, Treľová D, Kleščíková L, Lacík I, Rázga F. Dissociation of chitosan/tripolyphosphate complexes into separate components upon pH elevation. Carbohydr polym. 2018;192:104-110.

[21] Yoksan R, Chirachanchai S. Silver nanoparticle-loaded chitosan–starch-based films: Fabrication and evaluation of tensile, barrier and antimicrobial properties. Mater Sci Eng C. 2010;30(6):891-897.

[22] Obiweluozor FO, Emechebe GA, Tiwari AP, Kim JY, Park CH, Kim CS. Short duration cancer treatment: Inspired by a fast bio-resorbable smart nano-fiber device containing NIR lethal polydopamine nanospheres for effective chemo–photothermal cancer therapy. Int J Nanomed. 2018;6:375-390.

[23] Lísa M, Cífková E, Holčapek M. Lipidomic profiling of biological tissues using off-line two-dimensional high-performance liquid chromatography–mass spectrometry. J Chromatogr A. 2011;1218(31):5146-5156.

[24] D'Addio SM, Bothe JR, Neri C, Walsh PL, Zhang J, Pierson E, Mao Y, Gindy M, Leone A, Templeton AC. New and evolving techniques for the characterization of peptide therapeutics. J Pharm Sci. 2016;105(10):2989-3006.

[25] D'Souza G, Gross ND, Pai SI, Haddad R, Anderson KS, Rajan S, Gerber J, Gillison ML, Posner MR. Oral human papillomavirus (HPV) infection in HPV-positive patients with oropharyngeal cancer and their partners. J Clin Oncol. 2014;32(23):2408-2415.

[26] Tığlı Aydın RS, Pulat M. 5-Fluorouracil encapsulated chitosan nanoparticles for pH-stimulated drug delivery: Evaluation of controlled release kinetics. J Nanomater. 2012;2012(1):313961.

[27] Duraisamy S, Sathyan A, Balakrishnan S, Subramani P, Prahalathan C, Kumarasamy A. Bactericidal and non-cytotoxic activity of bacteriocin produced by *Lacticaseibacillus paracasei* F9-02 and evaluation of its tolerance to various physico-chemical conditions. Environ Microbiol. 2023;25(12):2882-2896.

[28] Joseph S, Kammann CI, Shepherd JG, Conte P, Schmidt HP, Hagemann N, Rich AM, Marjo CE, Allen J, Munroe P, Mitchell DR. Microstructural and associated chemical changes during the composting of a high temperature biochar: Mechanisms for nitrate, phosphate and other nutrient retention and release. Sci Total Environt. 2018;618:1210-1223.

[29] Ji J, Hao S, Wu D, Huang R, Xu Y. Preparation, characterization and in vitro release of chitosan nanoparticles loaded with gentamicin and salicylic acid. Carbohydr polym. 2011;85(4):803-808.

[30] Ziaee SA, Nejad FM, Dareyni M, Fakhri M. Evaluation of rheological and mechanical properties of hot and warm mix asphalt mixtures containing Electric Arc Furnace Slag using gyratory compactor. Constr Build Mater. 2023;378:131042.

[31] Manoj P, Watson DM, Neufeld DA, Megeath ST, Vavrek R, Yu V, Visser R, Bergin EA, Fischer WJ, Tobin JJ, Stutz AM. Herschel/PACS spectroscopic survey of protostars in orion: the origin of far-infrared CO emission. Astrophys J. 2013;763(2):8-13.

[32] Redah Alassaif F, Redah Alassaif E, Rani Chavali S, Dhanapal J. Suppressing the growth of HL-60 acute myeloid leukemia cells by chitosan coated anthraquinone nanoparticles *in vitro*. Int J Polym Mater Biomater. 2019;68(14):819-826.